



Electron transport through antidot superlattices in *Si/SiGe* heterostructures: new magnetoresistance resonances in lattices with large diameter antidots.

E. B. Olshanetsky, Vincent Thomas Francois Renard, Z.D. Kvon, J.-C. Portal, J.-M. Hartmann

► To cite this version:

E. B. Olshanetsky, Vincent Thomas Francois Renard, Z.D. Kvon, J.-C. Portal, J.-M. Hartmann. Electron transport through antidot superlattices in *Si/SiGe* heterostructures: new magnetoresistance resonances in lattices with large diameter antidots.. EPL - Europhysics Letters, 2006, 76 (4), pp.657. 10.1209/epl/i2006-10320-5 . hal-00097094

HAL Id: hal-00097094

<https://hal.science/hal-00097094>

Submitted on 21 Sep 2006

HAL is a multi-disciplinary open access archive for the deposit and dissemination of scientific research documents, whether they are published or not. The documents may come from teaching and research institutions in France or abroad, or from public or private research centers.

L'archive ouverte pluridisciplinaire **HAL**, est destinée au dépôt et à la diffusion de documents scientifiques de niveau recherche, publiés ou non, émanant des établissements d'enseignement et de recherche français ou étrangers, des laboratoires publics ou privés.

Electron transport through antidot superlattices in *Si/SiGe* heterostructures: new magnetoresistance resonances in lattices with large diameter antidots.

E. B. Olshanetsky¹, V. T. Renard^{2,3,*}, Z. D. Kvon¹, J. C. Portal^{2,3,4}, J. M. Hartmann⁵

¹ *Institute of Semiconductor Physics, Novosibirsk 630090, Russia;*

² *GHMFL, MPI-FKF/CNRS, BP-166, F-38042, Grenoble Cedex 9, France;*

³ *INSA-Toulouse, 31077, Cedex 4, France;*

⁴ *Institut Universitaire de France, Toulouse, France; and*

⁵ *CEA/Leti, F-38054, Grenoble, Cedex 9, France*

(Dated: 20 September 2006)

In the present work we have investigated the transport properties in a number of Si/SiGe samples with square antidot lattices of different periods. In samples with lattice periods equal to 700 nm and 850 nm we have observed the conventional low-field commensurability magnetoresistance peaks consistent with the previous observations in GaAs/AlGaAs and Si/SiGe samples with antidot lattices. In samples with a 600 nm lattice period a new series of well-developed magnetoresistance oscillations has been found beyond the last commensurability peak which are supposed to originate from periodic skipping orbits encircling an antidot with a particular number of bounds.

PACS numbers: 73.21.Cd, 73.23.Ad

I. INTRODUCTION

A two dimensional (2D) system modulated by a periodic strong repulsive potential is called an antidot lattice. Over the last 15 years various interesting phenomena have been observed in antidot lattices in uniform perpendicular magnetic fields. They are the low-field resonances in the longitudinal magnetoresistance, the corresponding non-quantized Hall plateaus and the quenching of the Hall effect near zero magnetic field,^{1,2,3,4,5,6}. These effects can be interpreted in terms of classical cyclotron orbits that are commensurate with the antidot lattice. A more thorough classical analysis based on the Kubo formula reveals that these effects have their origin in the magnetic field dependent mixture of chaotic and regular trajectories,^{7,8}.

Originally, all the antidot lattice related effects were observed in the interval between zero magnetic field and the field at which the last commensurability resonance $2r_c = a$ occurs, where r_c is the cyclotron radius and a is the antidot lattice period. Recently, however, it has become clear that under certain conditions a new type of longitudinal magnetoresistance resonances can be observed in antidot lattices at magnetic fields following the main commensurability peak $2r_c = a$ and before the beginning of the Shubnikov-de Haas oscillations,^{9,10,11}. Although the interpretation of these resonances is not yet fully developed, it is already clear that a large antidot diameter is necessary for their observation.

Experiments in antidot lattices usually require that the elastic mean free path of the electrons should be larger than the superlattice period. This explains why previously the majority of such experiments were carried out

in high mobility GaAs/AlGaAs heterostructures. Now, the progressively improving quality of the 2D electron gas in Si/SiGe heterostructures has made it an equally suitable material for the studies of electron transport in antidot lattices,¹².

In the present work we have investigated the transport properties of a number of square antidot lattices with different periods fabricated on top of a high mobility Si/SiGe heterostructure. In the samples with lattice periods 850 and 700 nm we observe the usual commensurability peaks and the shoulder-like feature at a higher field, already reported in¹². In the samples with the smallest lattice period (600 nm) a number of well developed and high-amplitude magnetoresistance oscillations are found in magnetic fields following the main commensurability peak $2r_c = a$. These new oscillations differ in certain respects from those reported in^{9,10,11} and are superior to them in size.

II. EXPERIMENTAL

Our samples were Hall bars fabricated on top of a *Si/Si_{0.75}Ge_{0.25}* heterostructure with a high mobility 2D electron gas,¹³. The distance between the potential probes was 100 μm ; the Hall bar width was 50 μm . The parameters of the original heterostructure were as follows: the electron density $N_s = (5.8 - 6) \times 10^{11} \text{cm}^{-2}$, the mobility $\mu = (1.6 - 2) \times 10^5 \text{cm}^2/\text{Vs}$. A square array of antidots with a lithographical diameter $d_l = 150 - 200 \text{nm}$, fabricated by electron beam lithography and reactive plasma etching covered the whole segment of the samples between the voltage probes. The total number of antidots was $(7 - 12) \times 10^3$. We have investigated six samples, two of each type, with different lattice periods equal to 600, 700 and 850 nm. The magnetoresistance was measured using a conventional four point ac lock-in scheme in a *He₃* cryostat at temperatures 0.3 - 4.2 K

*Present address : NTT Basic Research Laboratories, 3-1 Morinosato Wakamiya, Atsugi 243-0198, Japan

and in magnetic fields up to 13 T.

III. RESULTS AND DISCUSSION

Fig.1 shows a typical magnetoresistance dependence for sample *D18-01-10* with a 700 nm antidot lattice period. At low fields two commensurability peaks in the magnetoresistance curve can be observed. These well-known maxima were also found in the samples with the lattice period equal to 850 nm. Following these maxima there is a shoulder-like feature. At still higher fields Shubnikov-de Haas oscillations develop that can be used to determine the sheet electron density: $N_s = 5.3 \times 10^{11} \text{ cm}^{-2}$.

The positions of the low-field peaks are (1) - $B = 0.058 \text{ T}$ ($r_c/a \approx 1.75$) and (2) - $B = 0.233 \text{ T}$ ($r_c/a \approx 0.53$) respectively. Such peaks are also commonly observed in similar in size square antidot lattices on *AlGaAs/GaAs*,^{3,4,5,6}. Both the position and the magnitude of these peaks can be satisfactorily described by a model that takes into account two special types of regular electron trajectories in an antidot lattice. Namely, this model considers the contribution, on the one hand, of the so-called "pin-ball" trajectories localized around 1, 4 and more antidots (Ref.²) and, on the other hand, of the delocalized "runaway" trajectories that bounce away along a row of neighboring antidots, Ref.⁶. It is established that the relative contribution of the "pin-ball" and the "runaway" trajectories to the formation of the main commensurability peaks depends on the ratio d_e/a , where d_e is the antidot effective diameter and a is the lattice period. So, for $d_e/a < 0.5$ the contribution of the "runaway" trajectories dominates, while for $d_e/a \leq 1$ it is the "pin-ball" trajectories that give rise to the main commensurability peaks. In our case, peak 1 in Fig.1 must be due to "runaway" trajectories since in a lattice with the parameters of sample *D18-01-10* a "pin-ball" trajectory cannot give rise to a peak at the corresponding magnetic field.

The shoulder at $B = 0.376 \text{ T}$ ($r_c/a \approx 0.33$), that has also been observed in Ref.¹², will be discussed below.

In the Hall resistance (not shown) two additional non-quantized plateaus are observed at fields slightly higher than those of the commensurability peaks in ρ_{xx} . Around $B = 0$ the Hall effect is quenched.

The 700 and 850 nm samples are weakly sensitive to illumination which does not change noticeably the electron density and results only in a slight decrease of the zero field resistance. There is a weak temperature dependence of the commensurability oscillations below $T = 4.2 \text{ K}$. On the whole, apart from the shoulder, the behavior of the Si/SiGe samples with the antidot lattice periods 700 nm and 850 nm is found to reproduce the typical features well known from previous studies of GaAs/AlGaAs samples.

The situation, however, is different in the samples with the superlattice period 600 nm. The behavior of two such samples has been investigated. Fig.2a shows the charac-

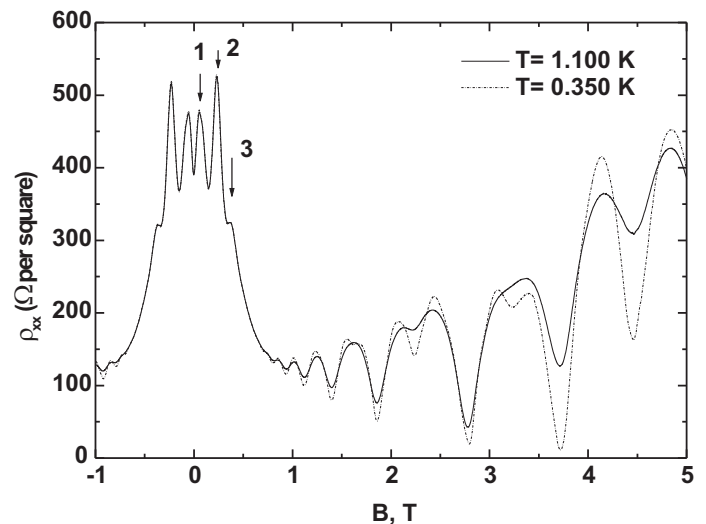


FIG. 1: Magnetoresistance in sample *D18-01-10* with a 700 nm lattice period. One can see two main commensurability peaks corresponding to (1) $r_c/a \approx 1.75$ and (2) $r_c/a \approx 0.53$ around zero field and a shoulder-like feature (3) at $r_c/a \approx 0.33$.

teristic MR curves obtained for sample *D18-01-07* after cooling down and without prior illumination. Although the zero field resistance ($\rho_{xx}(B = 0) \approx 23 \text{ k}\Omega$) is much higher than that of the 700 and 850 nm samples, the electron density estimated from the slope of the Hall resistance dependence is $N_s \approx 5.35 \times 10^{11} \text{ cm}^{-2}$, practically the same as in *D18-01-10* sample, Fig.1.

The peak *wl* at zero magnetic field is due to the suppression of the weak localization correction. The broad peak (1 : 2) at $B = 0.21 \text{ T}$ ($r_c/a \approx 0.64$) is supposed to be a superposition of the two main commensurability peaks similar to peaks 1 and 2 in Fig.1. Normally, no more commensurability features are expected at higher magnetic fields before the ShdH oscillations set in.

Nevertheless, in our 600 nm samples we observe at least three more peaks 3, 4, 5 at $B \approx 0.49$ ($r_c/a \approx 0.28$), 0.72 ($r_c/a \approx 0.2$) and 0.95 T ($r_c/a \approx 0.15$) respectively. The variation of the peaks 3, 4, 5 with temperature in Fig.2a is of the same order as that of the commensurability peak (1 : 2) showing them to be of a classical origin as well.

Fig.2a shows a high resistance state of a 600 nm sample. However, it was found that states of much lower resistance are possible in these samples with the new peaks still present. Fig. 3a shows the magnetoresistance of our second 600 nm sample *D18-01-08* that upon cooling down usually had a relatively low resistance state. One can see that despite more than a tenfold difference in zero field resistance the MR dependence in Fig.3a displays all the peculiar features observed in Fig.2a. Moreover, the position of the new peaks in magnetic field is the same as for the *D18-01-07* sample. The corresponding electron density estimated from the Hall resistance is $N_s \approx 5 \times 10^{11} \text{ cm}^{-2}$ which is slightly less than that for

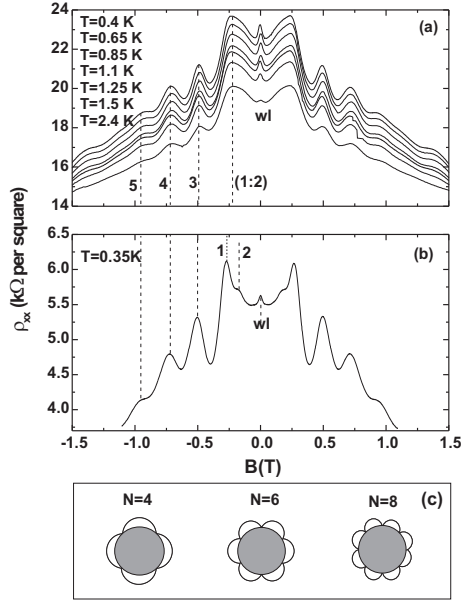


FIG. 2: Magnetoresistance of sample *D18-01-07* with the lattice period 600 nm (a)-before and (b)-after illumination. In (a) temperature increases from the upper to the lower curve. The dashed lines mark the position of the weak localization peak **wl**, the commensurability peaks **1, 2** and the new peaks **3, 4, 5**. (c)-schematic drawing of periodic skipping orbits with four, six and eight reflections from the antidot.

sample *D18-01-07* in Fig.2a. However, a precise determination of the electron density is difficult due to the deformation of the Hall resistance dependence in the 600 nm samples.

Fig.2b and 3b show the effect of illumination on the 600 nm samples. In both samples illumination results in a decrease of zero field resistance. At the same time within the experimental accuracy the electron density before and after illumination remains practically the same. Therefore, the change in resistance must be brought about by a mobility enhancement. This conclusion is also supported by the fact that in both samples the broad peak observed in the higher resistance state resolves itself after illumination into two conventional commensurability peaks **1** and **2**, Fig.2b,3b. The position of peaks **3, 4, 5** does not change with illumination.

The Hall resistance dependence in 600 nm samples is practically the same as in 700 and 850 nm samples with the quenching of the Hall effect and the additional plateaux corresponding to the commensurability peaks (see Fig.3c). No new features corresponding to the peaks **3, 4, 5** in $\rho_{xx}(B)$ have been found in the $\rho_{xy}(B)$ dependence.

To our knowledge there have been at least two experimental studies^{9,10,11} of magnetotransport in antidot superlattices where additional longitudinal resistance resonances were reported in magnetic fields following the last commensurability peak $2r_c = a$ and before the onset of Shubnikov-de Haas oscillations. In these experi-

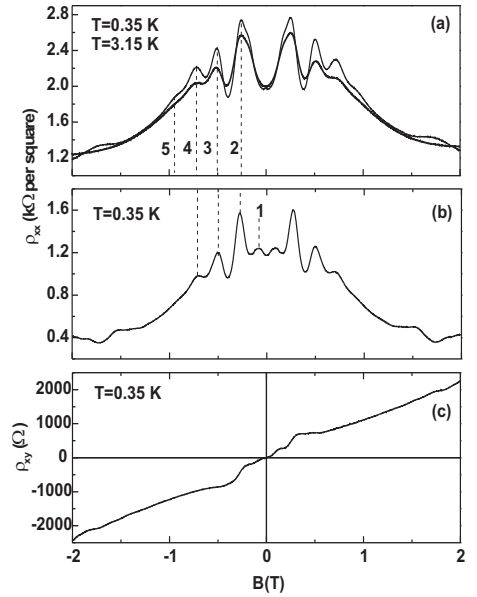


FIG. 3: Magnetoresistance of sample *D18-01-08* with the lattice period 600 nm (a)-before and (b)-after illumination. The numeration of the peaks is the same as in Fig.2. (c)-Hall resistance for the sample state after illumination (b).

ments the lattice was formed by large diameter antidots which seems to be crucial for the observation of the additional peaks. The single resonance observed in Ref.^{9,11} was supposed to be due to a localized electron trajectory locked in the free space pocket between four adjacent antidots. To describe this resonance a simple commensurability condition was suggested,^{9,11}: $2r_c = \sqrt{2}a - d_e$. The shoulder-like feature observed in our 700 nm samples (peak **3** in Fig.1) is likely to be of this kind. Indeed, applying to it the mentioned commensurability condition we obtain a reasonable value for the antidot effective diameter: $d_e \approx 540$ nm. This model, however, predicts only a single additional resonance and it fails in our 600 nm samples where a whole series of oscillations is observed after the main commensurability peak $2r_c = a$. In this case a more appropriate approach is the one used in Ref.¹⁰ where two additional broad peaks were reported.

The standard analysis performed in Ref.¹⁰ included evaluation of the Kubo formula that yields simulated magnetoresistance traces featuring the new peaks followed with the examination of Poincare sections allowing the identification of the electron trajectories responsible for the observed MR peaks. It has been shown that after the cyclotron radius becomes smaller than the distance between neighboring antidots a new class of electron trajectories becomes important that under certain conditions can give rise to a new type of magnetoresistance oscillations. In square lattices the new MR resonances are thought to arise due to rosette-shaped orbits that encircle the antidots and are localized similar to the pin-ball orbits responsible for the commensurability peak at $2r_c = a$. Also, it appears that contribution of such or-

bits to magnetoresistance depends on whether they are periodic, i.e. reproduce themselves on each revolution around an antidot, or non-periodic. It is the periodic rosette-shaped orbits, like those shown in Fig.2c, that give rise to individual maxima in magnetoresistance.

In our experiment the new peaks **3, 4, 5** lie at magnetic fields equal to 0.49, 0.72 and 0.95 T respectively. Assuming for simplicity the periodic skipping orbit of order N to be composed of N semicircles, we obtain the following simple geometric relation: $2r_c = d_e \sin(\pi/N)$, where d_e is the antidot effective diameter. Hence, $B_N \sim \sin(\pi/N)^{-1}$ is the magnetic field at which a magnetoresistance maximum corresponding to the periodic skipping orbit of order " N " is to be expected. Now, it is easy to show that the experimental maxima positions given above relate to each other in approximately the same way as B_N values corresponding to $N = 4, 6$ and 8 . Indeed, multiplying $\sin(\pi/N)^{-1}$ for $N = 4, 6$ and 8 by the same factor 0.346 , we obtain $0.49, 0.7$ and 0.91 in excellent agreement with the experimental maxima positions. So, we attribute the peaks **3, 4, 5** in Fig.2,3 to the periodic skipping orbits of order $N = 4, 6$ and 8 , shown in Fig.2c. This common factor 0.346 also gives us the antidot effective diameter d_e in the 600 nm samples. Indeed, taking $N_s = 5.35 \times 10^{11} \text{ cm}^{-2}$ we obtain $d_e \approx 490$ nm, which turns out to be more than two times larger than the lithographical size of the antidots. This value is also close to the effective diameter estimated from the position of the shoulder-like feature in the 700 nm period sample.

It is worth mentioning that the oscillations **3, 4, 5** observed in this work are very well developed and comparable in size to the main commensurability peak, far exceeding in this respect the features of this type observed so far. Moreover, comparing our results to¹⁰, where the experimental geometry was similar to ours, we find that whereas we resolve three peaks, identified as corresponding to $N = 4, 6$ and 8 , only two peaks $N = 4$ and $N = 8$ are reported in¹⁰ with peak $N = 6$ missing not only experimentally but in the calculation results as well. This and other facts raise a number of questions that we shall list here. First, it is still not very clear physically why periodic skipping orbits should be more efficient in trapping electrons around an antidot and thus giving rise to maxima in magnetoresistance than non-periodic skipping orbits. Also, it remains unclear why only periodic

skipping orbits of a certain order N should give rise to maxima in magnetoresistance, while others, say, $N = 5$ or $N = 7$, should have no such effect. Finally, as seen when comparing our results with Ref.¹⁰, the order N of peaks that one will observe seems to depend on particular experimental conditions. A possible explanation to the latter questions may be that the sample specific potential relief surrounding an antidot may be favorable to the formation of skipping orbits of certain orders N only.

Another important issue concerns our understanding of the antidot lattice parameters that favor the observation of the new oscillations. So far, it has been established that these oscillations can only be observed in lattices with a sufficiently large ratio d_e/a , although it is not quite clear why this should be important in the interpretation given above. In our case, these oscillations are present when $d_e/a \approx 0.8$ and are already absent in samples with $d_e/a \approx 0.7$. At the same time, in Ref.¹⁰, the oscillations are still observed in samples with $d_e/a \approx 0.7$. On the other hand, the steepness of the antidot potential does not seem to be an important factor. The new oscillations are present both in InAs/GaSb samples where the antidot effective diameter is almost equal to its lithographic size,¹⁰ and in our Si/SiGe samples where, due to the depletion effects, the effective diameter is more than two times larger than the lithographic diameter.

To conclude, we have investigated the transport properties of square antidot superlattices fabricated on Si/SiGe heterostructures. In lattices with a comparatively small ratio d_e/a (d_e is the antidot effective diameter, a is the lattice constant) we observe the usual commensurability maxima. In lattices with $d_e/a \approx 0.8$, apart from the usual commensurability peaks, we observe three well developed magnetoresistance resonances at higher magnetic fields. We attribute the new resonances to a successive formation of rosette-shaped orbits encircling an antidot and reflected from its boundary $4, 6$ and 8 times, respectively.

Acknowledgments

This work has been supported by RFBR project no. 06-02-16129 and by ANR PNANO MICONANO .

¹ K. Ensslin, P.M. Petroff Phys. Rev. B. **41**, 12307(R) (1990).

² D. Weiss, M.L. Roukes, A. Menschig, P. Grambow, K. von Klitzing, and G. Weimann Phys. Rev. Lett. **66**, 2790 (1991).

³ A. Lorke, J.P. Kotthaus, and K. Ploog Phys. Rev. B. **44**, 3447 (1991).

⁴ R. Schuster, K. Ensslin, J.P. Kotthaus, M. Holland, and C. Stanley Phys. Rev. B. **47**, 6843 (1993).

⁵ G.M. Gusev, V.T. Dolgoplov, Z.D. Kvon, A.A. Shashkin,

V.M. Kudriashov, L.V. Litvin, Yu.V. Nastaushv JETP Lett. **54**, 364 (1991).

⁶ G.M. Gusev, Z.D. Kvon, L.V. Litvin, Yu.V. Nastaushv, A.K. Kalagin, A.I. Toropov J.Phys.: Cond. Matter **41** L269 (1992).

⁷ E.M. Baskin, G.M. Gusev, Z.D. Kvon, A.G. Pogosov, M.V. Entin JETP Lett. **55**, 678 (1992).

⁸ R. Fleischmann, T. Geisel, and R. Ketzmerick Phys. Rev. Lett. **68** 1367 (1992).

⁹ M.V. Budantsev, Z.D. Kvon, A.G. Pogosov, J.C. Portal,

- D.C. Maude, N.T. Moshegov, A.E. Plotnikov, A.I. Toropov *Physica B* **260**, 363 (1998).
- ¹⁰ J. Eroms, M. Zitzlsperger, D. Weiss, J.H. Smet, C. Albrecht, R. Fleischmann, M. Behet, J. De Boeck, G. Borghs *Phys.Rev. B* **59**, 7829(R) (1999).
- ¹¹ Z.D. Kvon *JETP Lett.* **76**, 537 (2002).
- ¹² D. Tobben, M. Holzmann, S. Kuhn, H. Lorenz, G. Abstreiter, J.P. Kotthaus, F. Schaffler *Phys. Rev. B* **50**, 8853 (1994).
- ¹³ Hartmann J.M., Bogumilowicz Y., Holliger P., Laugier F., Truche R., Rolland R., Semeria M.N., Renard V., Olshanetsky E.B., Estibals O., Kvon Z.D., Portal J.C., Vincent L., Cristiano F., Claverie A. *Semicond. Sci. Technol.* **19**, 311 (2004).